EUROPEAN ORGANIZATION FOR NUCLEAR RESEARCH

THE STORAGE RING MAGNET OF THE THIRD MUON (g - 2) EXPERIMENT AT CERN

H. Drumm*) and C. Eck**)

Institut für Physik, Universität Mainz, Germany

G. Petrucci and Ö. Runólfsson

CERN, Geneva, Switzerland

ABSTRACT

The third (g - 2) experiment carried out at CERN required a storage ring magnet with a field as uniform as possible and known with an accuracy of a few parts per million over the whole storage region.

Here we describe this magnet, which has a useful aperture of 120 mm horizontally and 80 mm vertically and a diameter of $\sim$ 14 m.

The various field controls necessary are indicated, and the complex procedure adopted for the shimming work is described. The finally reached homogeneity of the field, averaged in azimuth, was 3 ppm.

All the various error sources and field map corrections needed are analysed.

Finally, the special aspects of the machine developed for the shimming are described.

Geneva - 1 June 1978

(Submitted to Nuclear Instruments and Methods)

---

*) Now at the Physikalisches Institut der Universität Heidelberg, Germany.

**) Now at CERN, Geneva, Switzerland.

1. INTRODUCTION

The storage ring magnet described in this paper was designed and built for the third experiment[1-3] carried out at CERN to determine the muon (g - 2) anomaly[a].

This anomaly is related to the precession of the spin with respect to the momentum vector of particles moving in a magnetic field according to the formula

$$\omega_a = \omega_{spin} - \omega_c = \frac{g-2}{2}\left(\frac{e}{mc}\right) B = a\left(\frac{e}{mc}\right) B ,$$

where a is the anomaly parameter, B is the magnetic field seen by the particles, ω_{spin} and ω_c are the angular rotation frequencies of the spin and the momentum vector; m is the particle mass, and e and c are the electron charge and the light velocity.

The experiment was done by storing muon particles in a storage ring where they were circulating. The anomaly is deduced from the knowledge of B and the measurement of ω_a [b].

The accuracy of the (g - 2) determination thus depends strictly upon the accuracy of the knowledge of B.

In order to improve this accuracy as much as possible, the storage ring magnet for the third (g - 2) experiment was designed and shimmed for a fixed muon momentum (p = 3.098 GeV/c) and a magnetic field as uniform as possible[c] over the entire storage ring[4]. This ring had a storage volume with an average diameter of 14 m, and horizontal and vertical apertures of 120 mm and 80 mm, respectively. The field value was 1.47 T. The vertical focusing forces necessary to keep the muon circulating were provided by electrostatic quadrupoles[5], which do not affect the relative spin motion (ω_a) because of the very particularly chosen muon momentum[d].

Figure 1 gives the general layout of the experiment. Protons interact in a target (at the right of the figure) from which a secondary pion beam is generated. These pions are injected into the ring through a pulsed inflector*) (septum) magnet

*) G. Lebée, unpublished.

presenting a very low stray field in the storage volume, and cross the storage volume over more than half the ring's circumference. During this time some of them decay, and a small fraction of the muons produced are trapped in stable orbits. This method of injection assures a high degree of polarization and a low background.

Figure 2 is a photograph showing the storage ring itself.

2. THE DESIGN OF THE MAGNET

The product of the diameter and average magnetic field of the ring was determined by the desired γ value of the muons. The best field value was found by studying a half-scale model of two magnet blocks. The chosen field of 1.47 T, corresponding to a ring diameter of 14 m, enabled a very homogeneous field to be obtained throughout a sufficiently large aperture (Fig. 3), using a reasonably sized magnet, without running into difficulties due to excessive saturation.

The ring was actually a polygon made out of 40 identical C-shaped magnet blocks, with their opening directed towards the centre of the ring. Each block (Fig. 3) consisted of five pieces of solid, forged, low-carbon steel: two pole pieces, 1.1 m long, and three rectangular yoke pieces, 1 m long. The pole pieces were tapered by 4.5° at both ends to form, as far as possible, a continuous ring, this continuous structure being essential to the precise determination of the magnetic field (Table 1). The conical slots between the blocks were necessary to accommodate the coil supports and cooling water connections. The optimum pole profile was determined by a trial and error method on the half-scale model. The blocks were delivered by the factory, having been machined with the smallest possible tolerances on the dimensions of the magnet gap and the pole profile (Fig. 4). The tolerances required on this profile and on the parallelism of the two surfaces when the block was charged by a force equal to the magnetic force in operation (40 tons) were ±0.02 mm.

Care was taken to design the magnet for optimum stability and reproducible mounting; therefore the contact surfaces between the poles and the yoke pieces were limited to well-defined and precisely ground strips. Dowels were used to

determine the precise relative position of the block pieces. In this way the imposed tolerances could be kept over several remounting operations.

The magnet was energized by four large continuous coils made from hollow copper conductor (Figs. 2, 3, and 5). The two larger ones, of about 15 m diameter, produced essentially the magnetic field in the gap. The two smaller ones, of 13 m diameter, compensated the stray field, which would otherwise have been strong and probably a source of serious difficulties that would interfere in the control of the magnet, as well as in the operation of the experiment. All four coils were connected in series to the rectifier.

Because of their dimensions, each coil was made up of five sectors, in which each individual conductor was cooled by a separate water circuit. The water flow had the same direction in all circuits to keep the temperature gradients in all coils as low as possible. Corresponding conductors of different sectors were electrically connected by laminated flexible copper joints (Figs. 6 and 7) to form a complete circular coil. The cooling of these connectors was achieved through contact with the rigid conductors of the sector, and the temperature of the connectors was about 10°C above the conductor temperature. Owing to the particular fragility of these joints, the end of each one was equipped with a thermistor, and an automatic unit kept all 960 thermistors under permanent surveillance during the operation of the magnet. If a thermistor value exceeded the preset high or low limits, the magnet current was switched off, and the fault position and status were stored and displayed. This security system proved to be very efficient in the event of bad contacts, short circuits, or insufficient cooling in any of the 480 parallel cooling circuits.

Very good stability and control of the magnetic field, as well as geometrical stability of the magnet parts far beyond that which is usual in the accelerator field, were required by this experiment. The magnet system was erected on a solid, temperature-stabilized, concrete ring, which in turn rested on five pillars erected on the underlying rock, approximately 10 m below. The temperature of the experimental hall was kept constant to about ±1°C, and the temperature and pressure

of the cooling water were also stabilized. The maximum temperature rise between the water inlets and outlets was limited to 10°C.

Each magnet block was positioned, to within a few hundredths of a millimetre, by means of three special jacks*). These consisted of cylinders, each of them filled with soft polyurethane on which rested a piston transmitting the load. The pistons were moved by compressing the polyurethane by means of bolts. On these jacks four further bolts were provided to assure horizontal adjustment and clamping of the blocks. The position of each block was controlled by optical and mechanical survey devices mounted on a pillar in the centre of the ring.

The coils were supported, independently of the magnet blocks, by 20 C-shaped stainless-steel supports (Fig. 3); in this way, the positioning of each block did not disturb the others and, in addition, the unavoidable thermal expansion of the coils did not affect the blocks. This thermal expansion was absorbed by the laminated connectors, thus avoiding radial displacement that otherwise might be a source of uncontrollable field variations.

3. FIELD CONTROL

In order to assure the desired magnetic field stability and a sufficiently close control of its value, a number of precautions were necessary. The magnet was powered by a 12-phase thyristor rectifier, and passive and active filters[6] reduced the current ripple to a negligible level. Its current stability was a few ppm short-term, and better than 100 ppm long-term. The rectifier was switched on following a hardware-programmed pattern (Fig. 8) in order to reduce hysteresis effects. The field level in each block was fixed by means of a permanently installed nuclear magnetic resonance (NMR) system[7] (see Fig. 13). Its error signal was fed through a power amplifier to a pair of thin coils wound around the poles of the block. The crystal-controlled frequency fed to the magnetometer was selected such that the average field in each block was within 50 ppm from the nominal field value. For this a set of eight crystal oscillators of different frequencies

*) D. Bois, unpublished.

was needed. A pick-up coil was placed in the gap of each block in order to obtain stable operation of the control loop, the pick-up signal being added to the NMR error signal. A few blocks around the inflector magnet were stabilized using error signals from neighbouring blocks. The sum of all error signals was used to control the rectifier current setting.

Periodically the magnet was carefully mapped by NMR servomagnetometers. The effects of the vacuum tank and all other components installed in the magnet were measured at the beginning and at the end of the experiment.

During the data-taking, the actual field values inside the storage volume were sampled every few hours by means of so-called plunging probes[7]. These probes were servomagnetometers mounted in vacuum-tight sleeves on the vacuum tank. They were moved radially into the useful aperture of the magnet, and their positions and readings were recorded by the data acquisition system of the experiment. There was a plunging probe in every block, except at the inflector where it was replaced by a fixed magnetometer. Comparison of the plunging-probe readings with the complete field map permitted a precise survey of the magnetic field during the experiment.

4. SHIMMING THE RING MAGNET

A considerable amount of shimming was necessary in order to obtain the average homogeneity of a few ppm. The difficulty of this task was eased by the fact that the magnet was designed to work only at a fixed field value. Therefore no active corrections, such as pole-face windings, were necessary and we could restrict the work to passive shimming. Almost any desired field correction could be obtained by removing iron from the pole face, and the desired average field value could be restored by adding iron shunts on the yoke. Small field variations in the azimuth were of no importance to the (g - 2) experiment. Therefore, provided one took care not to leave big local gradients, which might have been difficult to map by NMR, it was sufficient to apply corrections to the field map after averaging over azimuthal sections. This simplified the problem to a two-dimensional

one, which could be treated by the on-line computer[8], a PDP 11/20 with a disk-operating system. Before final shimming of the assembled ring took place, all 40 magnet blocks were adjusted and shimmed in a 5 m long coil (see Fig. 17) shaped and curved as a section of the ring. For this set, where four blocks were mounted, the following adjustments were required[9]:

i) The two end blocks were equipped with pole pieces of a length adjusted to minimize the magnetic flux passing between the pole ends of the centre and end blocks. In this way, end effects, which were absent in the assembled ring, were eliminated, as far as possible, from the two central blocks.

ii) Iron shunts (Fig. 3) mounted on the open side of the magnet yoke reduced the radial gradient, which was mainly due to saturation of the yoke, from about 2×10^{-2} to less than 10^{-4} across the useful aperture.

iii) The azimuthal field variations were reduced from about $\sim 1.5 \times 10^{-2}$ to about 2×10^{-4} by introducing wedge-shaped steel pieces (Fig. 3) into the space between the yokes of neighbouring magnets, and by making slots between the pole and the yoke, near the centre of each block (Fig. 3). These slots were partly filled in again with thin sheets of steel to minimize azimuthal field variations.

iv) The average field in all blocks was equalized by adding steel shunts on the top and bottom surfaces of the horizontal yoke. This adjustment was made individually on each block before the final shimming, using the end blocks as references.

Following these initial adjustments, the central blocks were then shimmed individually. Of the several shimming methods tried on the half-scale model, the most adequate was found to be that of removing thin strips from the pole surface by means of a grinding tool.

In a successfully shimmed block, the radial gradient averaged over the azimuth in the median plane was required to be not more than a few 10^{-5} across the aperture, and the weighted r.m.s. deviations from the mean value less than 15 ppm.

Usually one or two cycles of measurements and grinding were sufficient. The 40 blocks of the magnet were shimmed at a rate of two per week; this included the three days needed to exchange the blocks.

For some not fully understood reasons, the field shape obtained by the first shim process was not sufficiently well reproduced in the assembled ring. Therefore the procedure described above had to be repeated on the assembled ring. The final result of the vertical plane averaged over all 40 blocks is shown in Fig. 9. The r.m.s. value of the field differences, and the r.m.s. value weighted with the muon distribution over the measured grid of 9 × 13 points in the radial vertical plane of the field, were 15.3 ppm and 3.2 ppm, respectively.

Care was taken not to leave low-order multipoles in the field distribution, as this might cause beam losses. This was done by choosing the correct field level in each block (Fig. 10), and by shimming the ring to eliminate low-order gradients in the radial vertical field map, averaged over short sections in azimuth. Eventual losses of stored muons were determined entirely by the quality of the electric quadrupole field (Refs. 5 and 10).

Although it would not have been too difficult to improve these results still further (again repeating the same procedure), this was considered unnecessary since errors in the experimental measurements, due to the field shape, became negligible compared with the obtainable statistical error.

The calculation for the final shimming was done in the following way[11]. One of the two central blocks was mapped, on a dense grid (10 × 10 × 40 mm) covering the useful aperture, by eight NMR magnetometers mounted on a numerically controlled scanner (see Fig. 17). From this map, three average radial vertical field maps were calculated, one from a 700 mm long section of the centre, and two from 200 mm long sections of each end. The shim corrections for each map were found by minimizing the field differences on 28 representative points (Fig. 4). The shims were chosen so as to produce a homogeneous field where most of the stored muons (about 90%) would be found, without giving too much weight to the border of the aperture where the particle density would be low. The model used treated the

shims as azimuthally infinite current loops, together with their images in two infinite and perfect mirrors in the pole planes. The program handled up to 16 loops of fixed radial dimension, normally 20 mm, equal to the grinding-wheel width, at eight predetermined radial positions. This problem was represented by a set of 28 linear, normally independent equations of 17 variables, the 16 shim thicknesses and the magnet current, of the form

$$\frac{\Delta B}{B_0}\left(r_i,z_i\right) = \frac{1}{\pi}\sum_{s=1}^{16} t_s\left(r_i - r_s + b_s\right)\sum_{I=1}^{8}\frac{1}{\left[z_i+z_s(2I-1)\cdot(-1)^I\right]^2+\left(r_i-r_s+b_s\right)^2}$$

$$-\frac{1}{\pi}\sum_{s=1}^{16} t_s\left(r_i - r_s - b_s\right)\sum_{I=1}^{8}\frac{1}{\left[z_i+z_s(2I-1)\cdot(-1)^I\right]^2+\left(r_i-r_s-b_s\right)^2} + A\cdot\Delta J\ ,$$

where r_i,z_i are the radial and vertical coordinates of the 28 representative points; r_s and z_s are the radial and vertical coordinates of the 16 shim (loops) positions; b_s and t_s are the half-width and the thickness of the shims, respectively; I labels the mirror images included in the calculation (eight images were calculated by the program); ΔJ is the main current change; and, finally, A is proportional to the slope of the excitation curve at the nominal field.

The solution consisted in finding the combination of shim thicknesses t_s and current change ΔJ minimizing the root mean square of the field deviations. The procedure followed was to set $\Delta B(r_i,z_i)$ equal to but of opposite sign from the measured field variations at the selected positions (r_i,z_i), and then to determine t_s by the method of least squares fits. The shim position (r_s,z_s) and the shim half-width b_s were fixed. These were normally selected by the operator from among a few sets of standard combinations.

The resulting shim thicknesses, the predicted r.m.s., and the weighted r.m.s. deviations of all 117 points on the field map were printed. A display routine produced field contour maps showing lines of equal field strength generated by linear interpolation between mesh points. It was possible to display results of

measurements and calculations as well as to add and subtract maps. The choice between different solutions depended on the predicted r.m.s. values, the appearance of the field map, and the convenience of the required profile modifications.

5. EVALUATION OF THE FIELD MAP FOR THE (g - 2) EXPERIMENT

In order to evaluate the field map for the experiment, it was necessary to know everything affecting the field measurements and the field shape after the measurements. The relation between the measured field map and the control measurements obtained during physics runs by monitoring probes (plunging probes) had to be established.

This was done in the following way[12]:

i) A calibration magnetometer of well-defined geometry and known susceptibility correction δ^{cal} was prepared.

ii) The magnetometers on the measuring machine were calibrated against the calibration magnetometer; usually a secondary standard probe was used. This calibration $\delta^{map}(r,z,\theta)$ included the effect of the measuring machine on individual probes.

iii) The change in field shape $\delta^{stab}(r,z,\theta)$ due to the effect of the measuring machine on the stabilization magnetometer was determined.

iv) The effects $\delta^{vac}(r,z,\theta)$ of the vacuum tank and of all other components including the inflector stray field, which were not present when the magnet was mapped, were determined.

v) The effect of the vacuum tank on all stabilization magnetometers was measured. This effect modified the field map $\delta^{v-stab}(r,z,\theta)$ in the opposite direction.

vi) The magnet was mapped repeatedly to follow the initial drift with time and obtain a precise field map $f(r,z,\theta,t)$.

vii) The field $f^{pp}(r,z,\theta)$ at the positions of all plunging probes was measured separately after the magnet had stabilized.

Because the field was homogeneous and all corrections were small, the corrected field map $f^0(r,z,\theta,t)$ could be expressed as

$$f^0(r,z,\theta,t) = f(r,z,\theta,t)\left[1+\delta^{cal}+\delta^{map}(r,z,\theta)+\delta^{stab}(r,z,\theta)+\delta^{vac}(r,z,\theta)+\delta^{v\text{-}stab}(r,z,\theta)\right] .$$

The corresponding expression for the corrected value $f^{0PP}(r,z,\theta)$ at the plunging-probe position was obtained by replacing $f(r,z,\theta,t)$ by $f^{PP}(r,z,\theta)$ in the above formula.

The reproducibility of the average field level was found to be about ±1 ppm. Applying all above-mentioned corrections point by point and averaging over several maps and data runs, the agreement between the measured field map and the field map calculated from the plunging-probe measurements was at the level of a few 10^{-7}. This provided a good check of the procedure adopted.

Experience showed that the average field measured at the plunging-probe positions varied in time very similarly to the average field of the magnet. The reason was that the plunging probes, which traversed the centre of the aperture, gave a better representation of the average field than did the stabilization probes located outside the vacuum tank. After an initial drifting for about three days, the average field remained stable at a level of 1 ppm. A typical behaviour of the average field is shown in Fig. 11. The time-dependent field value to be used for the data analysis was then obtained according to the formula

$$f(t) = \frac{\left[\overline{f^0(r,z,\theta,t=0)\cdot W(r,z)}\cdot\overline{P(t)}\right]}{\overline{f^{0PP}(t=0)}} ,$$

where $t = 0$ refers to the field map before the run, and $P(t)$ is the calibrated mean value of all plunging-probe measurements. The bars indicate averaging over all coordinates. The weight function $W(r,z)$ is proportional to the time-averaged muon density in an rz plane, assuming that their distribution in phase space is homogeneous; it is given by the expression

$$W(r_i,z_i) = \frac{\sqrt{(r^2_{max}-r^2_i)\cdot(z^2_{max}-z^2_i)}}{\sum_i \sqrt{(r^2_{max}-r^2_i)\cdot(z^2_{max}-z^2_i)}},$$

where r_{max}, z_{max} are the borders of the useful aperture.

The average field level during the experiment is shown in Fig. 12; the X were obtained from the field maps, the curves from plunging-probe measurements. The big jumps occurred when the temperature stabilization of the cooling water failed. Values of various corrections are listed in Table 2.

6. MAPPING TECHNIQUE

The magnet was mapped by a computer-controlled machine (Fig. 13), pivoting on the central pillar of the ring and rolling on the lower magnet pole. The position of the eight NMR probes was controlled by three incremental encoders. The encoder for the azimuthal position was mounted on the axis of one of the wheels rolling on the magnet pole. Absolute position control was obtained by end switches and photoelectrical sensing of a reference pin on each magnet. The useful aperture of the magnet was mapped on a 10 × 10 mm grid in the radial vertical plane (Fig. 4), and at intervals of 0.164° in the azimuth. The total of 257,400 measurements was obtained in seven hours.

The 4 m long vacuum chambers were mapped by sliding them over a set of NMR probes, mounted on a 5 m long free-standing arm in the homogeneous region of the magnet. The chambers were displaced by means of the measuring machine. The measured field variations represented directly a map of the effect of the chambers.

The effect of the vacuum system and other materials on the stabilization probes was obtained by replacing the stabilizing magnetometer with a servomagnetometer, and reading the field variations when the vacuum chamber was moved in and out of the magnet gap.

7. MAPPING THE HORIZONTAL COMPONENTS OF THE MAGNETIC FIELD

The radial component of the magnetic field was measured a few times during the experiment, either by a flip-coil method[13] or by a Hall-plate pendulum[14] at a limited number of points (120 to 360 points). A typical result is shown in Fig. 14.

Both methods gave consistent results. The first was reproducible to a tilt level of a few 10^{-6} radians, the second to about 10^{-5} radians. Locally the maximum observed tilt of the field vector with respect to the vertical was 3×10^{-4} radians. During the experiment the average value over the ring fluctuated between $\pm 50 \times 10^{-6}$ radians. The effective median plane of the stored beam was shifted vertically in proportion to the average value of the first harmonic of the radial component. This reduced the useful aperture of the ring by a few millimetres.

This instability of the field direction was observed independently by detectors that were sensitive to the beam position in the experiment[15]. No effort was made to determine the source of this small instability.

The azimuthal component of the field was found to be less than 10^{-3} of the main component everywhere inside the storage volume. The value of (g - 2) obtained in the experiment was insensitive to this component since its integral effect for one revolution is zero.

8. GRINDING

As it is an unconventional technique to grind the poles of an assembled magnet in order to correct a measured field shape, we will describe in some detail the tool developed for this purpose. Tests on the half-scale model magnet permitted the determination of the criteria for successful grinding of the soft-iron pole surface without use of a liquid. The important points were:

- the choice of quality of the grinding wheel;
- efficient evacuation of the products of grinding;
- periodical dressing of the grinding-wheel surface;

- low working pressure of the grinding wheel on the pole surface;
- vibration-free displacement of the grinding wheel;
- a precise control of the metal removed.

Other essential features of the grinding tool were: it fitted into the magnet gap and could easily be moved in and out. It could grind off in a short time azimuthal strips 150 mm long, 20 mm wide, and up to a few tenths of a millimetre thick, with a precision of a few microns. Its operation was safe enough to avoid any accidental damaging of the pole surface.

The grinding tool is shown schematically in the following figures: Fig. 15, side view; Fig. 16, outside the magnet; Fig. 17, in its working position.

The grinding wheel was mounted on a spindle and rotated at 3000 turns/min, pulled by an axially mounted three-phase motor. The spindle support was mounted on the moving part of a linear bearing (on which the stone could be displaced radially across the magnet gap) by means of a manually operated lead screw. The radial position was read on a numerical display connected to an encoder on the lead screw. The fixed part of the linear bearing was mounted on a pivot with the axis in the radial direction. A hydraulic cylinder was used to raise or lower the grinding wheel, the range of vertical movement being limited by a pair of micrometers acting on the long lever arm of the pivoting part. The lever arm also carried weights to counterbalance the spindle and the motor. The pivot was mounted on the end of a rigid frame; the azimuthal sides of the frame were made of the mobile parts of a pair of linear bearings, the fixed part of which was mounted on the base plane. A second hydraulic piston displaced the frame in the azimuthal direction.

The base plate was equipped with retractable wheels, rolling on the shims of the magnet. The machine was moved in and out of the magnet and from one working position to another on these wheels. The wheels, as well as the strong jack on the top of the base plate that served to clamp the tool in the magnet gap, were actuated pneumatically. A rail, mounted at a fixed distance on the lower coil

outside the magnet and parallel to the block, guided the tool when it was rolling to the working position. Its azimuthal position was read off a graduated ruler on this rail. The link between the base plate and the rail was made by means of two pairs of guide wheels fixed on extensions of the base plate.

A system consisting of switches, relays, and pneumatic logic, moved the spindle sequentially down-forward-up-back. The bottom and the top poles were thus shimmed simultaneously, at the same position, in analogy to the procedure of the program that calculated the shim thicknesses. The working pressure of the wheel was controlled by the oil pressure of the pivoting cylinder. Needle valves in the oil circuit were used to control the speed of displacement and served to damp vibrations.

The only critical operation was the setting of the strip thickness to be removed by grinding. To obtain precise settings, the system was first started and the motor switched on with low torque. The two micrometers were then slowly turned until the grinding wheel started to produce sparks. Then the micrometers were turned to a setting corresponding to the strip thickness to be removed, using the first reading as zero. Once this adjustment was done the motor was switched to normal power.

The typical time taken to remove a strip 15 cm long, 2 cm wide and 0.01 cm thick was 15 minutes. By taking some care, a precision of ±5 μm was achieved. The agreement between the calculated and measured effects of shims agreed perfectly within the precision to which a shim could be measured, i.e. at a few microns.

The grinding was done without the use of any liquid, which would have been very inconvenient for an assembled magnet. The products of the grinding were collected in a metal box, surrounding the grinding wheel, which was connected to a vacuum cleaner.

The most frequently used grindstone quality was PA46-K8-V40W from the Carborundum Company. Its surface was periodically dressed by a diamond.

Acknowledgements

The authors would like to thank the other members of the (g - 2) team for continuous help throughout the construction of the magnet. They also wish to acknowledge the contribution of many of their CERN colleagues in the accomplishment of this task: in particular, G. Lebée was responsible for the general installation and the geometrical survey of the magnet; L. Baisin and R. Pintus were responsible for the drawings of the magnet and the grinding machine; B. Danner and J. Buttkus provided for the operation of the high-stability power supply; F. Cataneo developed the plunging probes, and J. Lindsay implemented the associated electronics; A. Orève designed the unit which surveyed the junction temperatures of the main coil; K. Mühlemann and G. Frémont built the NMR probes and the electronics for the magnetic field control.

Finally, particular thanks are due to A. Uldry, M. Esteban and P. Knobel, who have worked hard and conscientiously to mount the magnet and the measuring and grinding devices, and have supplied invaluable help throughout all the complex shimming and mapping operations.

NOTES

a) The first muon (g - 2) experiment made at CERN, using a straight 6 m long magnet, obtained the value $(1162 \pm 3) \times 10^{-6}$ for the anomaly parameter $a = (g - 2)/2$; the second one, using a 5 m diameter weak focusing storage ring, gave the value $(116616 \pm 31) \times 10^{-8}$. The third experiment, using the magnet described in this paper, finally gave the value $a = (1165924 \pm 8) \times 10^{-9}$, i.e. an accuracy of 7 ppm.

b) The precession ω_a is measured, using special counters to record the instantaneous rate of electrons produced above a given energy in the decay of the circulating muons. This rate varies in time as a function of the instantaneous direction of the muon polarization.

c) In the previous experiment using a conventional weak focusing ring, the error in the estimate of (g - 2) due to the uncertainty (about ±3 mm) in the muon distribution inside the storage volume was of the order of 160 ppm, i.e. more than one order of magnitude larger than the final error aimed at for this third experiment.

d) The expression of ω_a in the presence of magnetic and electrostatic fields perpendicular to the particle motion is given by

$$\omega_a = \frac{e}{mc}\left[aB + \left(\frac{1}{\gamma^2 - 1} - a\right)\beta \cdot E\right].$$

The second term of this expression vanishes for $\gamma = 29.3$, i.e. for the chosen 3.098 GeV/c momentum. Corrections due to momentum spread are small and easy to apply.

REFERENCES

1) G. Charpak, F.J.M. Farley, R.L. Garwin, T. Muller, J.C. Sens and A. Zichichi, Nuovo Cimento 37 (1965) 1241.

2) J. Bailey, W. Bartl, G. von Bochman, R.C.A. Brown, F.J.M. Farley, M. Giesch, H. Jöstlein, S. van der Meer, E. Picasso and R.W. Williams, Nuovo Cimento 9A (1972) 369.

3a) J. Bailey, K. Borer, F. Combley, H. Drumm, C. Eck, F.J.M. Farley, J.H. Field, W. Flegel, P.M. Hattersley, F. Krienen, F. Lange, G. Petrucci, E. Picasso, H.I. Pizer, Ö. Runólfsson, R.W. Williams and S. Wojcicki, Phys. Letters 55B (1975) 420.

J. Bailey, K. Borer, F. Combley, H. Drumm, F.J.M. Farley, J.H. Field, W. Flegel, P.M. Hattersley, F. Krienen, F. Lange, E. Picasso and W. von Rüden, Phys. Letters 67B (1977) 225.

3b) J. Bailey, K. Borer, F. Combley, H. Drumm, C. Eck, F.J.M. Farley, J.H. Field, W. Flegel, P.M. Hattersley, F. Krienen, F. Lange, G. Lebée, E. MacMillan, G. Petrucci, E. Picasso, W. von Rüden, Ö. Runólfsson, R.W. Williams and S. Wojcicki, The anomalous magnetic moment of the muon, detailed paper in preparation.

4) J. Bailey, F.J.M. Farley, H. Jöstlein, G. Petrucci, E. Picasso and F. Wickens, CERN Proposal PH I/COM-69/20 (1969).

5) W. Flegel and F. Krienen, Nuclear Instrum. Methods 113 (1973) 549.

6) N. Rasmussen, CERN/MPS/ED 73-1 (1973).

7) K. Borer, Nuclear Instrum. Methods 143 (1977) 203.

8) B. Hedin, The Program MINMIN, unpublished.

9) K.C. Eck, Ph.D. Thesis, University of Mainz, Germany, 1974.

10) J. Bailey, K. Borer, F. Combley, H. Drumm, F.J.M. Farley, J.H. Field, W. Flegel, P.M. Hattersley, F. Krienen, F. Lange, E. Picasso and W. von Rüden, Nature 268 (1977) 301.

11) H. Drumm, Ph.D. Thesis, University of Mainz, Germany, 1976, and CERN EP Internal Report 77-12 (1977).

12) K. Borer and F. Lange, Nuclear Instrum. Methods 143 (1977) 219.

13) R.C.A. Brown, CERN 69-8 (1969), p. 33.

14) N.K. Abrasimov, V.A. Eliseev and G.A. Ryabov, Device for the measurement of the median plane position (Leningrad, 1967) [CERN Trans. 71-5 (1971)].

15) J. Bailey, K. Borer, F. Combley, H. Drumm, F.J.M. Farley, J.H. Field, W. Flegel, P.M. Hattersley, F. Krienen, F. Lange, E. Picasso and W. von Rüden, Nuclear Phys. 4 (1978) 345.

Table 1

Parameters of the magnet

Diameter: 14 m
Aperture: 380 × 140 mm^2
Useful aperture: 120 × 80 mm^2
Structure: 40 identical C-shaped blocks
Total weight: 450 t
Four main coils, two of 13 m diameter, two of 15 m diameter
Each coil 24 turns, subdivided into five sectors, connected by 480 flexible connectors
Conductor: electrolytic copper, 28 × 30 mm^2 with 8 mm Ø bore
Coil weight: 30 t
Current: 4200 A; excitation power: 2 MW
480 cooling water circuits
Water flow: 60 m^3/h; pressure drop: 3 bar
Temperature rise 10°C; inlet stabilized at 25°C
80 small compensating coils
Nominal field: 1.47 T
Field variation in the useful aperture: $\Delta B/B < \pm 300$ ppm
Weighted r.m.s. field variations for the experiment: 3 ppm
Stability: ±1 ppm
Reproducibility: short term, ±1 ppm long term, a few ppm
Field control: 1 ppm
Low-order multipole components negligible
Average field direction: vertical $\pm 50 \times 10^{-6}$ radians

Table 2

Values of the correction applied to the field measurements

Susceptibility correction of the reference probe δ^{cal}:	25.1 ± 0.1 ppm
Calibration of individual magnetometers on the machine δ^{map}:	-0.1 ± 0.5 ppm
Correction due to the perturbation of the stabilization by the measuring machine δ^{stab}:	-1.5 ± 0.2 ppm
Corrections due to the vacuum tank and inflector: δ^{vac}:	+2.8 ± 0.4 ppm
δ^{v-stab}:	-2.8 ± 0.4 ppm

Figure captions

Fig. 1 : Layout of the muon storage ring and beam line.

Fig. 2 : General view of the ring.

Fig. 3 : A magnet block (dimensions in mm):

(A) front view

(B) side view of a block, the coils, and their supports

(C) top view

C : main coils

CC : compensating coils

P : contact surfaces between block parts

S : shunts to adjust the field level

SL : slots to reduce the azimuthal field variation

W : wedges to reduce the field variation at the junction of neighbouring blocks

RS : shunts to reduce the radial field gradient.

Fig. 4 : Cut through the aperture (dimensions in mm). The initial shim dimensions are given at the top pole. The most frequently used positions of the final shim corrections are indicated at the bottom pole. The useful aperture and the grid for the field map is indicated. The X are the points used to calculate the shim corrections. The dashed lines are the extreme positions of the beam aperture relative to the pole pieces.

Fig. 5 : View of the partly assembled ring. The end of a coil section with its water inlets is visible, as well as a correction coil on the lower pole piece.

Fig. 6 : A flexible connector. The solid end blocks are electron-beam-welded to the laminated conductor. The thermistor housing is soft-soldered to the solid block. The connector is mounted on the coil by two pairs of M6 screws. The contact surfaces are silver plated.

Fig. 7 : Assembled flexible coil junction.

Fig. 8 : The switching-on procedure of the magnet.

Fig. 9 : A vertical field map, shown as a contour line plot for the storage aperture obtained by averaging a three-dimensional map in azimuth. The points lie on a square grid of 1 cm spacing, and the lines, which connect up points of equal field strength, are obtained by linear interpolation. The interval between contours is 2 ppm, which is equivalent to about 3 μT.

Fig. 10 : Field variations around the ring. The average value of each block is plotted.

Fig. 11 : Typical behaviour of the average field, obtained from plunging-probe measurements during a long physics run. The results of nine complete field maps obtained during five days before the runs are marked by (X). Note the good agreement between the two measurements during the initial drift period, and the good stability of the average field afterwards.

Fig. 12 : Variation of the average field during the experiment. X are results of complete field maps. The curves are obtained from the plunging-probe measurements during physics runs. The variations in November 1975 and August 1976 are probably due to failures in the cooling-water temperature control which occurred at those times.

Fig. 13 : The mapping machine. The NMR probes are shown in the magnet gap, and some of the motors and position encoders are also visible. On the left of the picture a stabilization probe, mounted in position on the upper pole piece, can be seen. The measuring probes are arranged to permit measurement of the complete useful aperture with the stabilization probe in position in the median plane of the gap.

Fig. 14 : Azimuthal variation of the tilt of the field vector, measured in the centre of each block. The curves are the average value and the first harmonic of their radial field component.

Fig. 15 : A schematic side-view of the grinding tool.

Fig. 16 : The grinding tool with the control rack.

Fig. 17 : The grinding tool in its working position in the four-block set-up. The numerically controlled scanner is visible in the foreground.

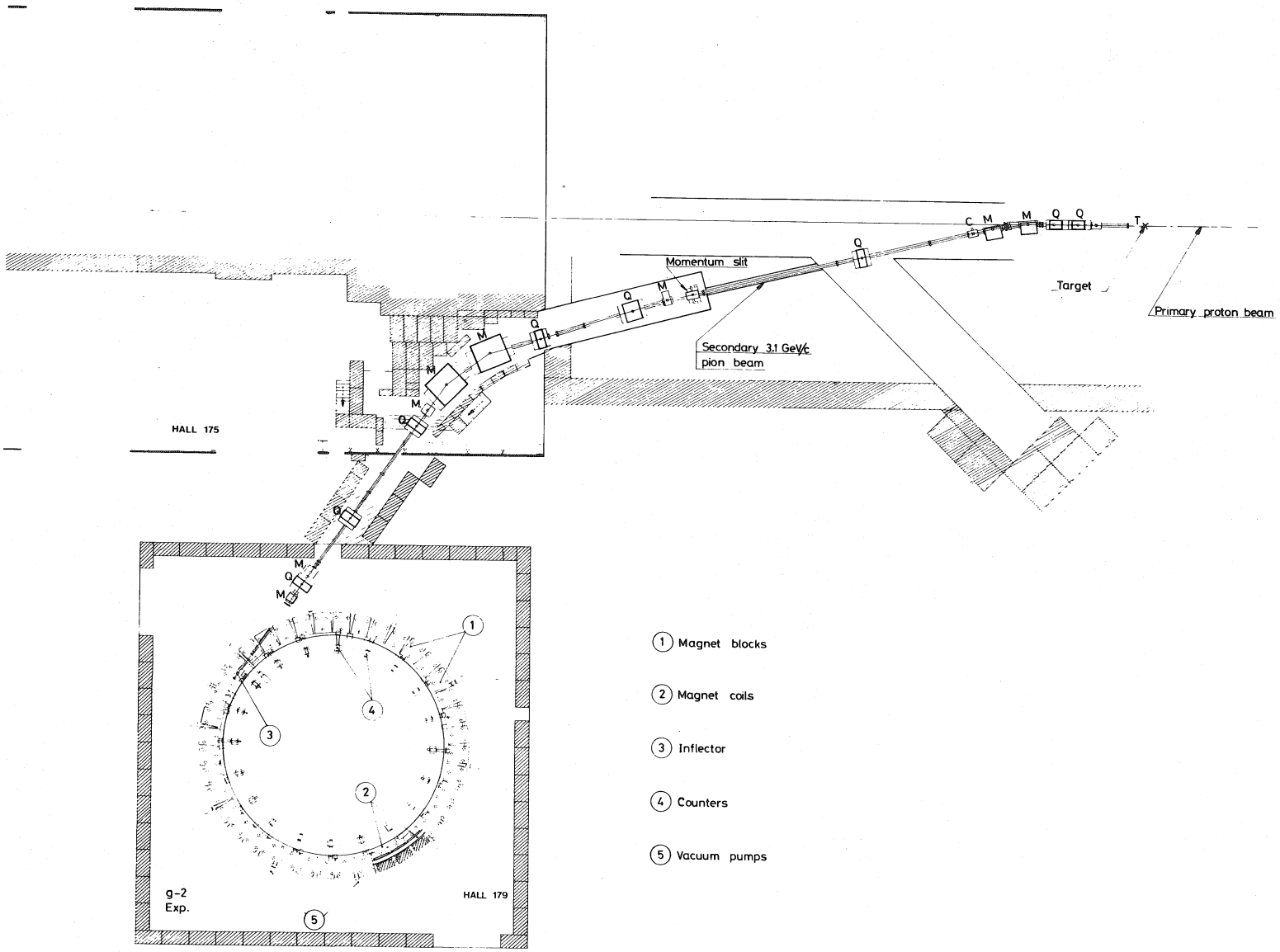
C M M Q Q T
Q
Momentum slit
Q
M
Q
M
Target
Primary proton beam
Secondary 3.1 GeV/c
pion beam
M
M
Q
HALL 175
Q
M
Q
M
1
4
3
2
g-2
Exp.
HALL 179
5
1 Magnet blocks
2 Magnet coils
3 Inflector
4 Counters
5 Vacuum pumps

Fig. 1

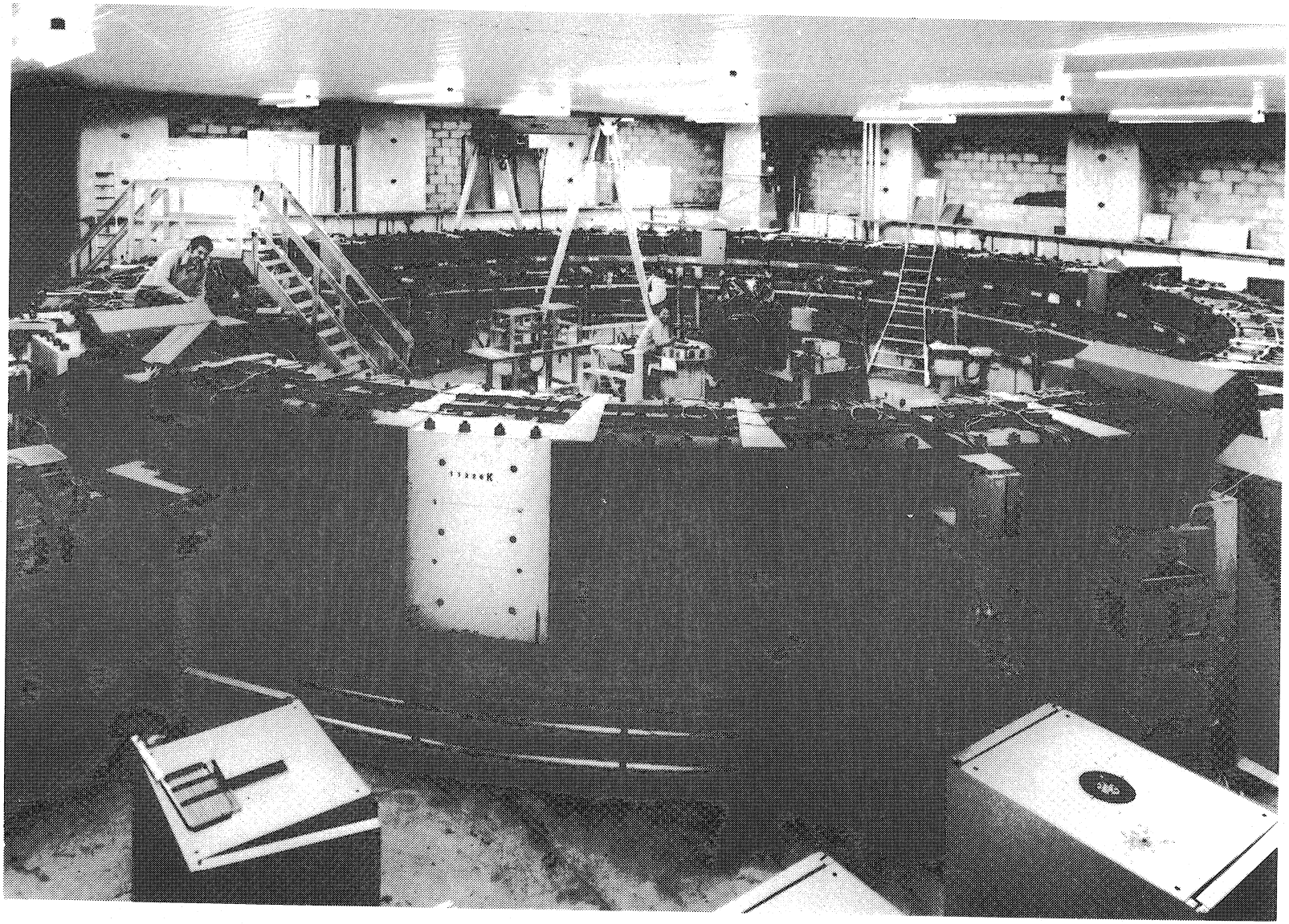

Fig. 2

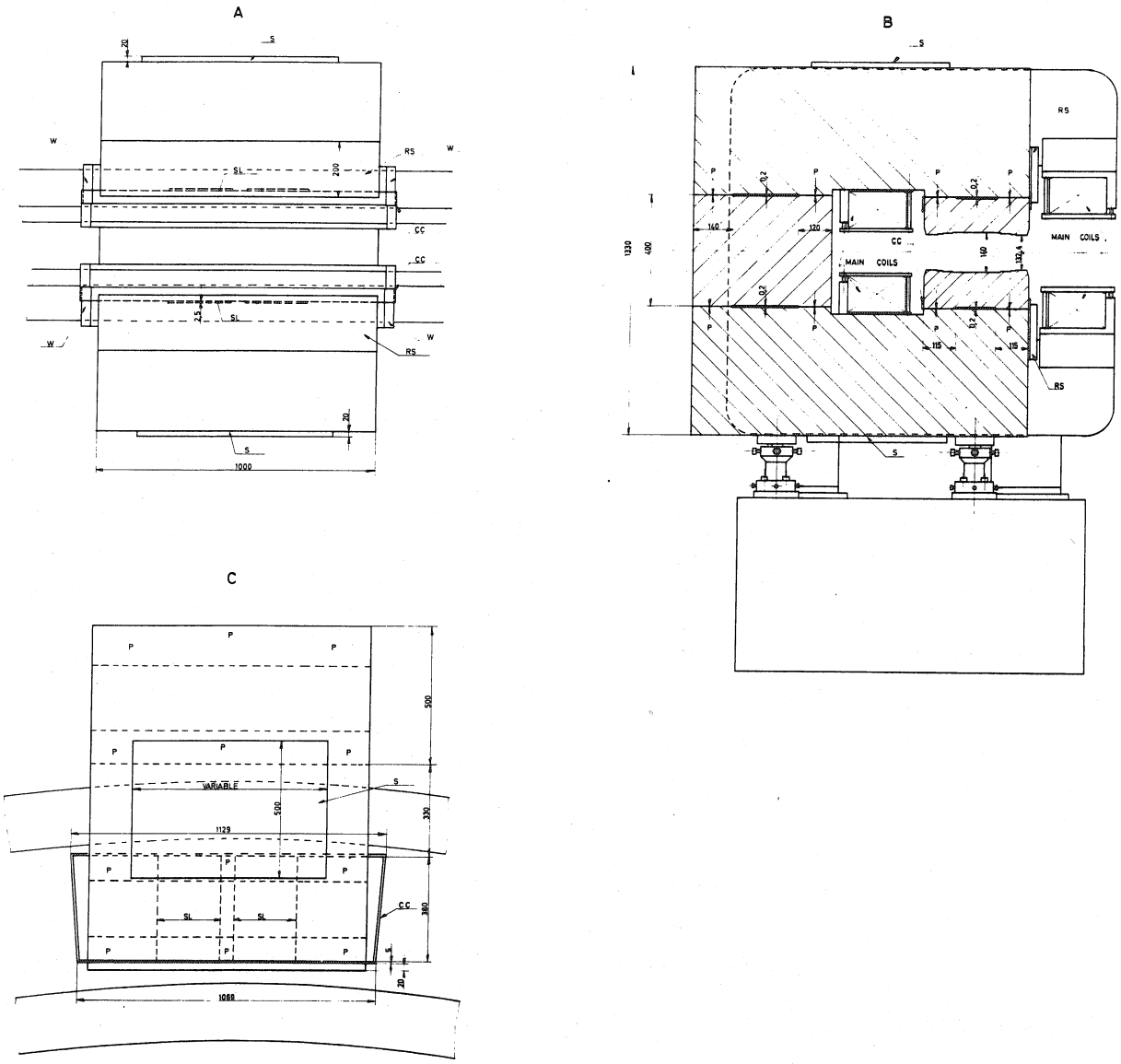

Fig. 3

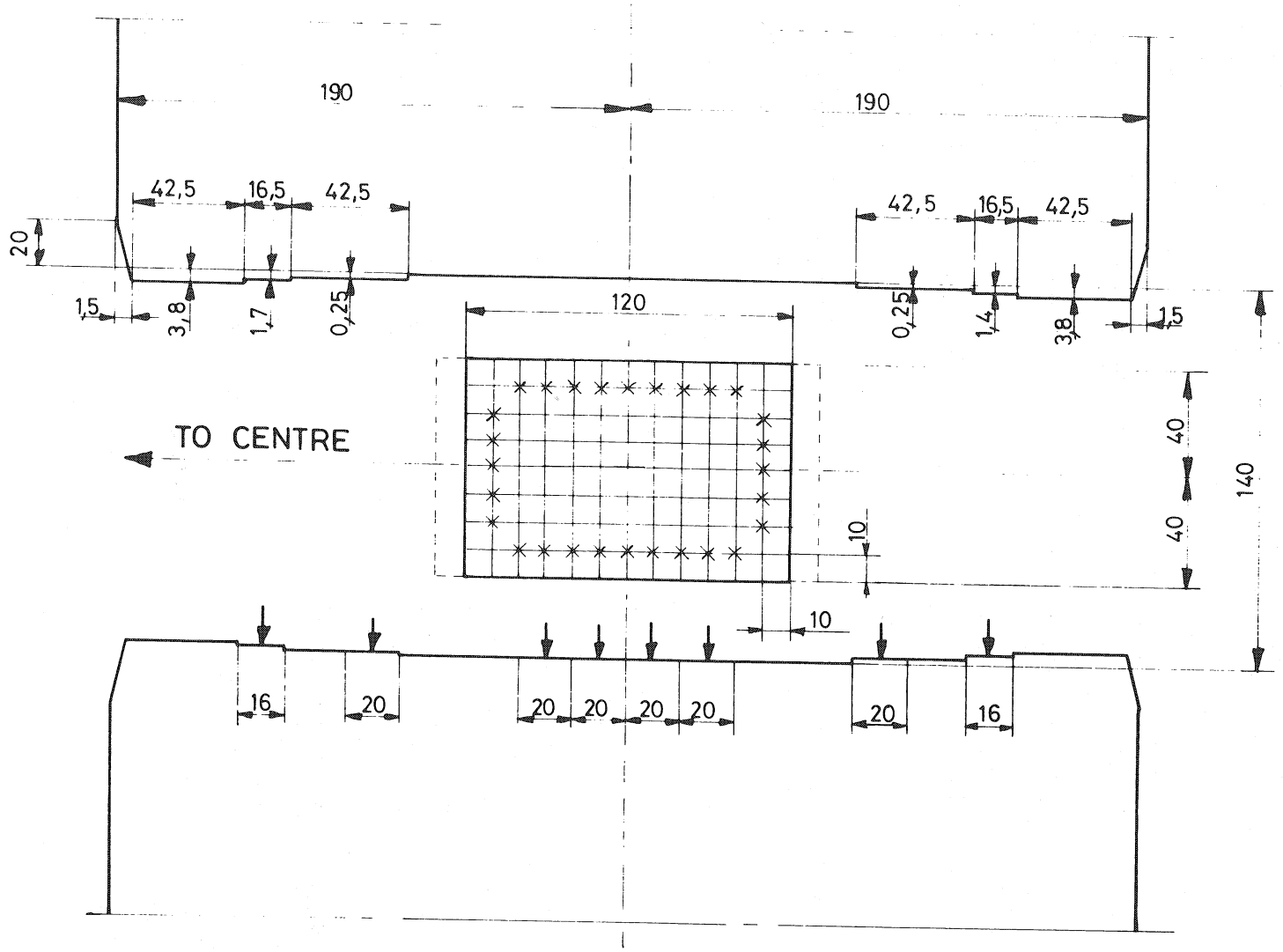
190
190
42,5
16,5
42,5
42,5
16,5
42,5
20
1,5
3,8
1,7
0,25
120
0,25
1,4
3,8
1,5
TO CENTRE
40
40
140
10
10
16
20
20
20
20
20
20
16

Fig. 4

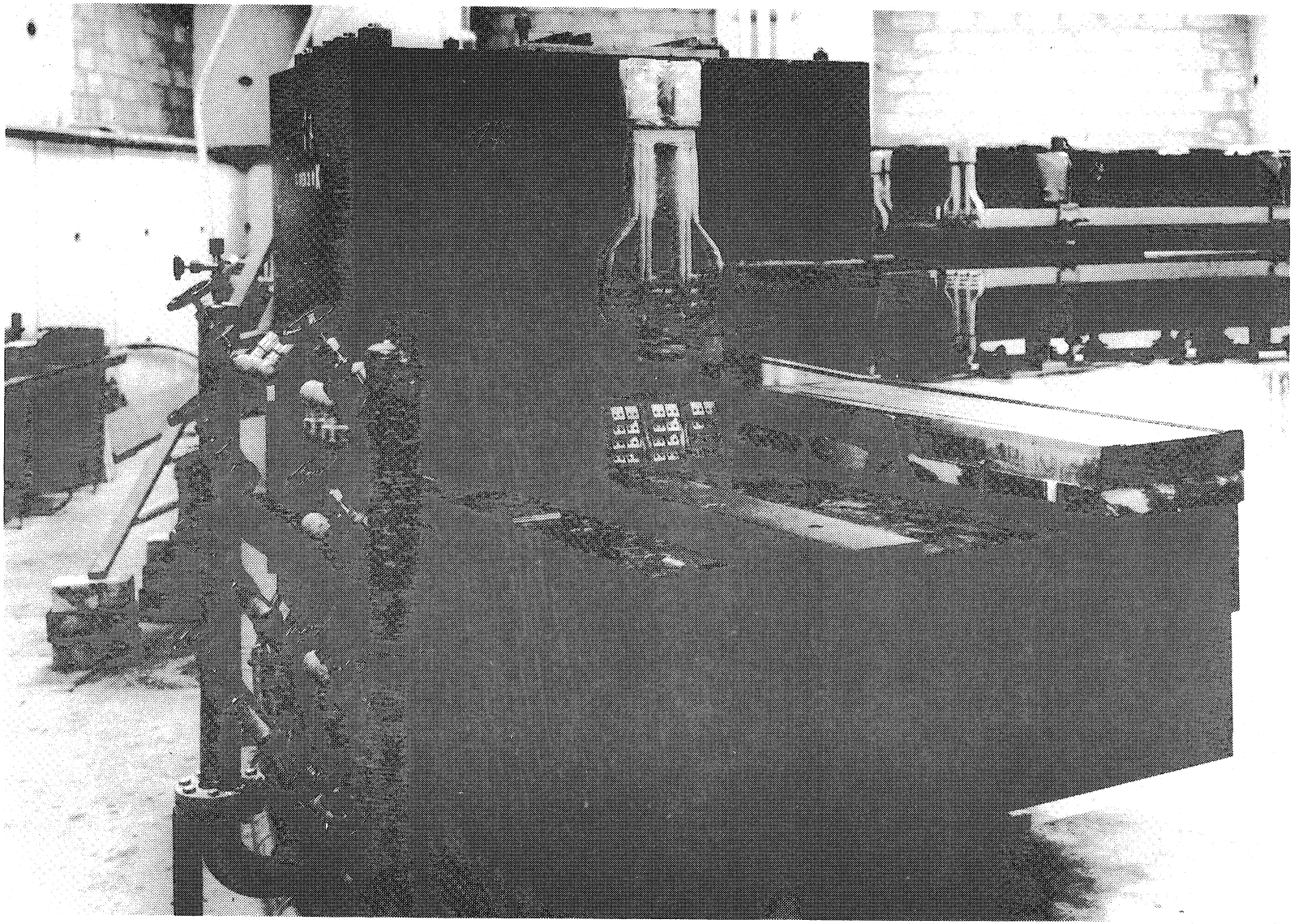

Fig. 5

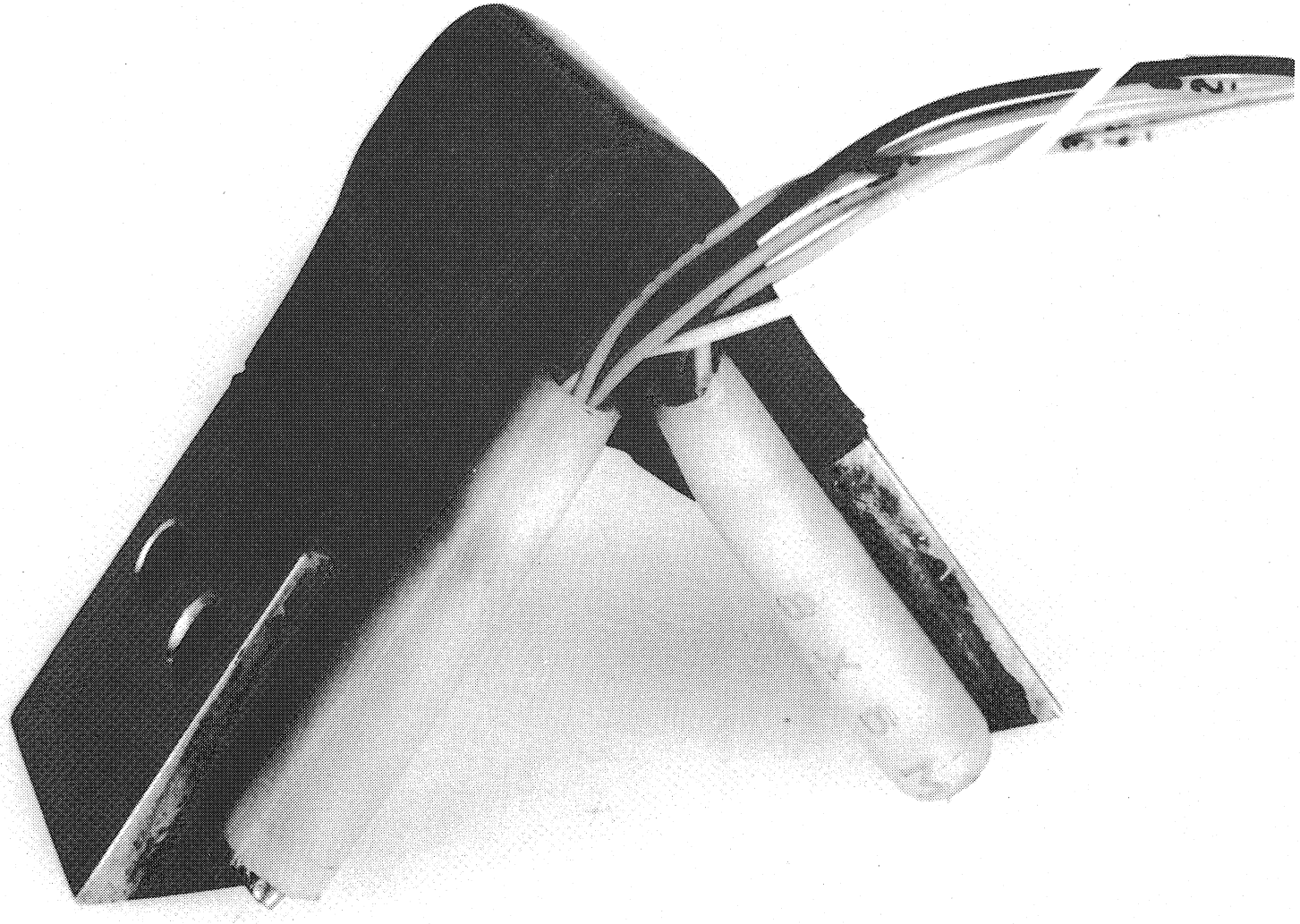

Fig. 6

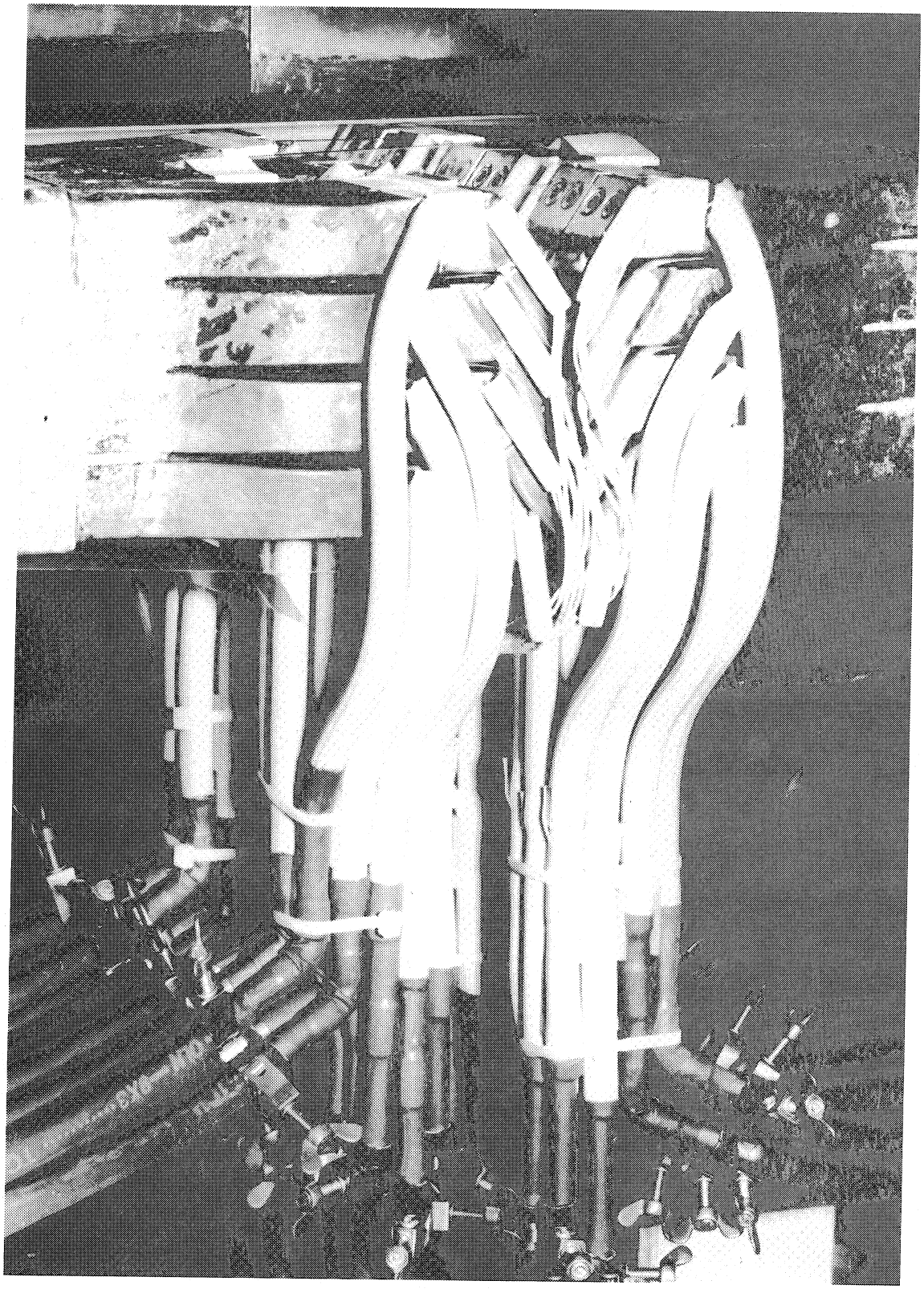

Fig. 7

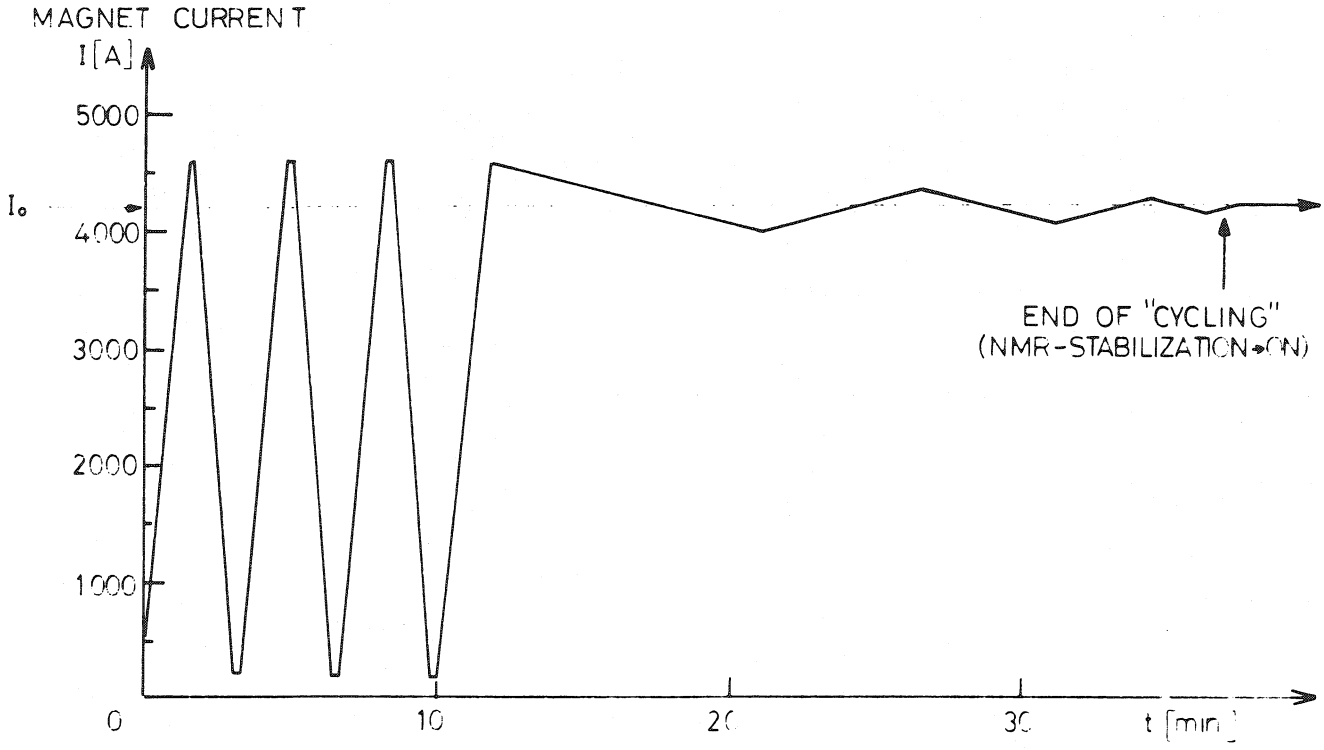
MAGNET CURRENT
I[A]
5000
I_o
4000
3000
2000
1000
0
10
20
30
t [min]
END OF "CYCLING"
(NMR-STABILIZATION→ON)

Fig. 8

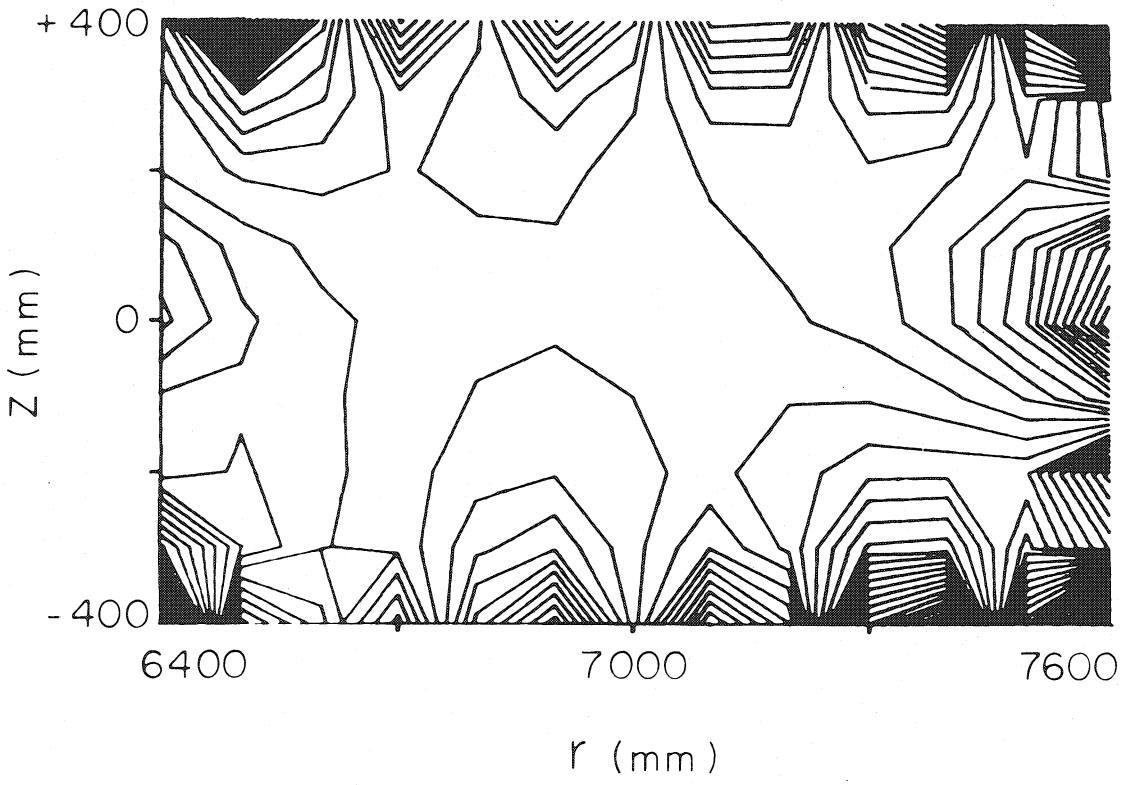
+400
0
-400
Z (mm)
6400
7000
7600
r (mm)

Fig. 9

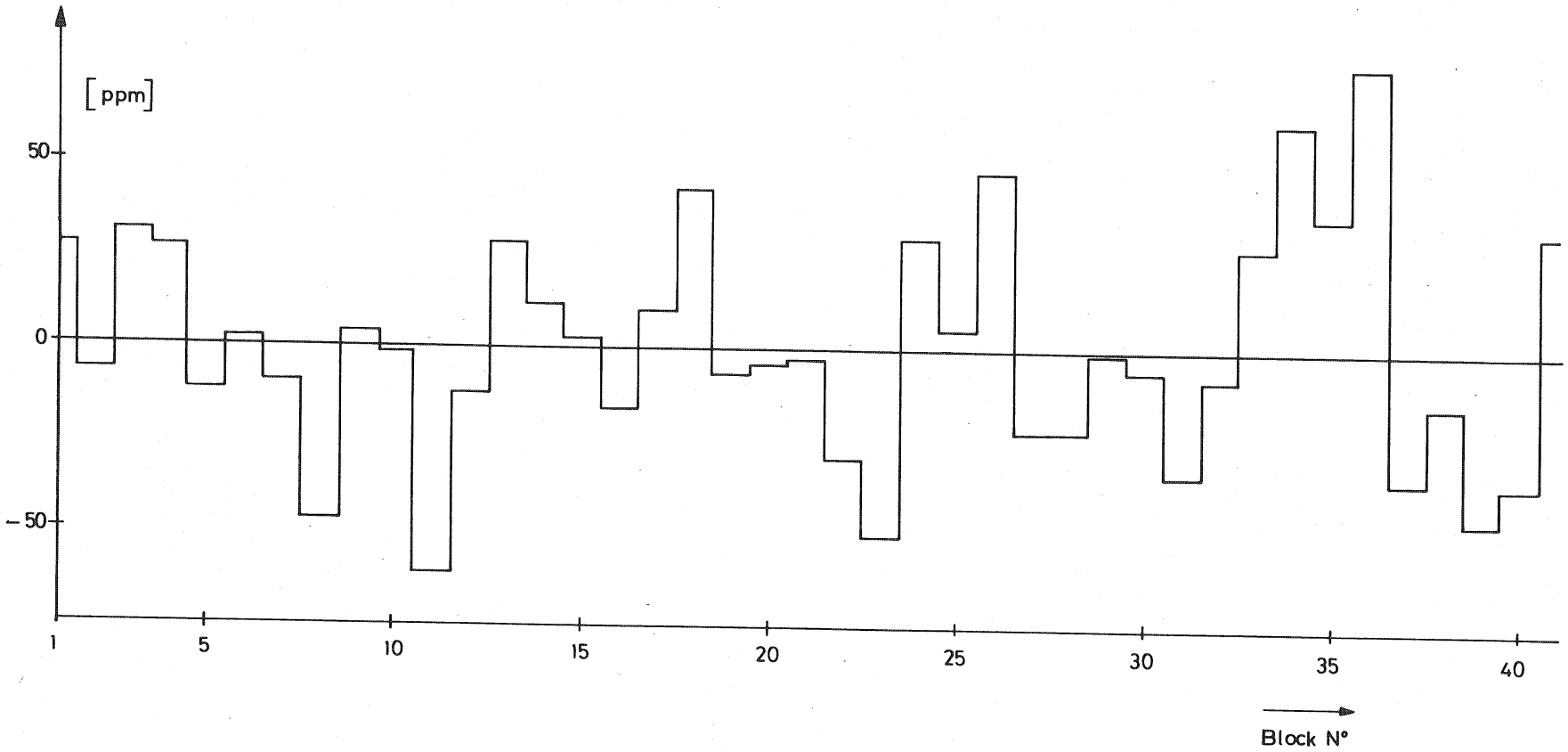

Fig. 10

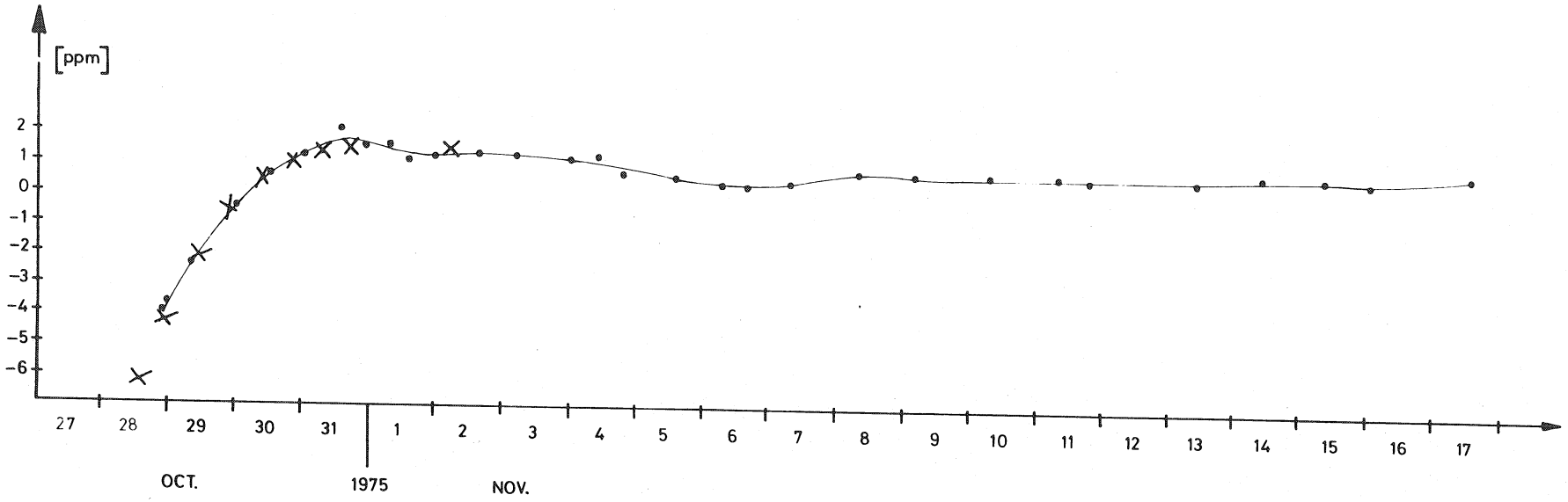
[ppm]
2
1
0
-1
-2
-3
-4
-5
-6
27
28
29
30
31
1
2
3
4
5
6
7
8
9
10
11
12
13
14
15
16
17
OCT.
1975
NOV.

Fig. 11

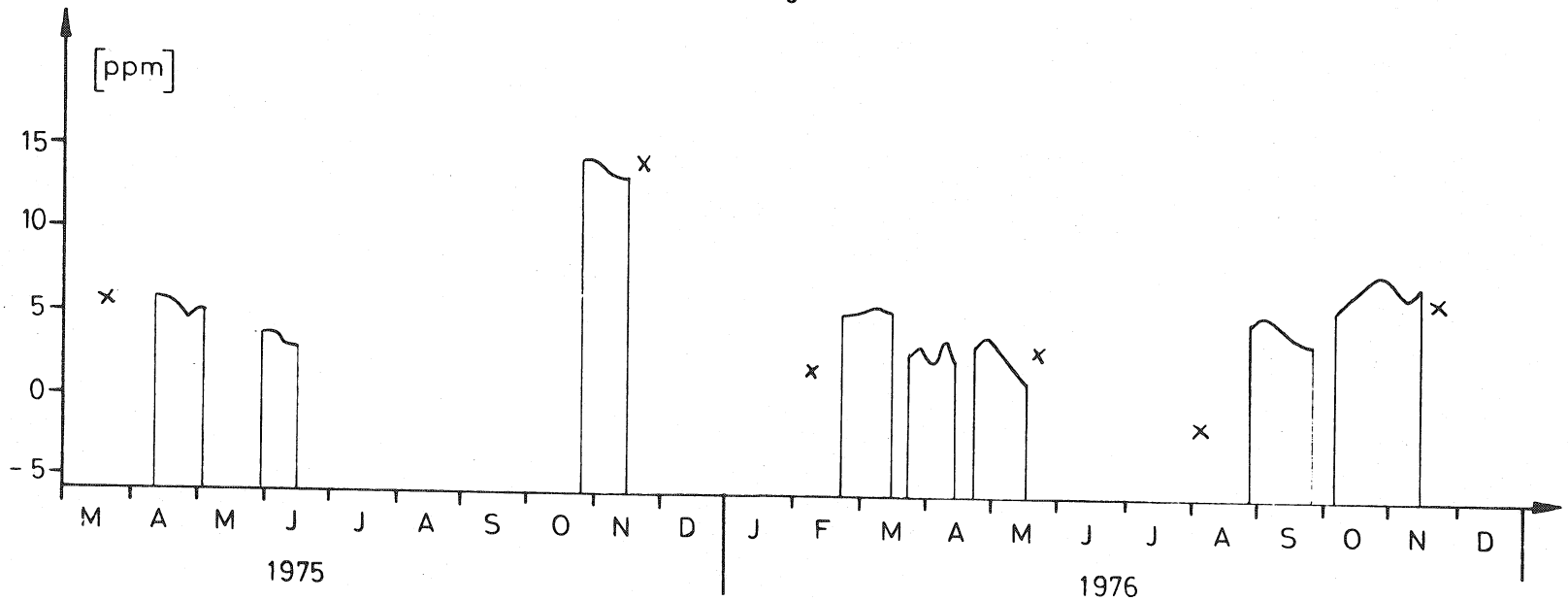
[ppm]
15
10
5
0
-5
M
A
M
J
J
A
S
O
N
D
J
F
M
A
M
J
J
A
S
O
N
D
1975
1976

Fig. 12

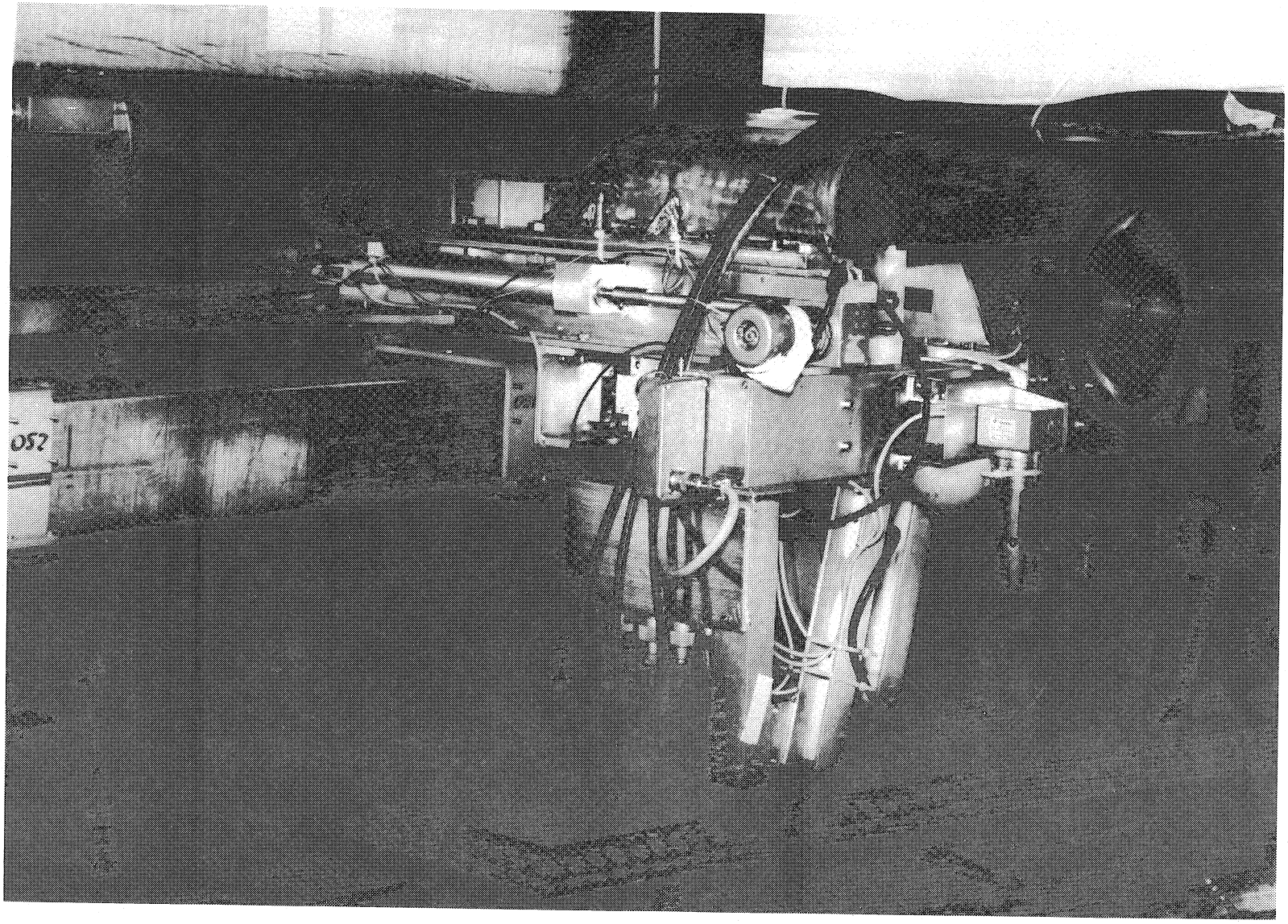

Fig. 13

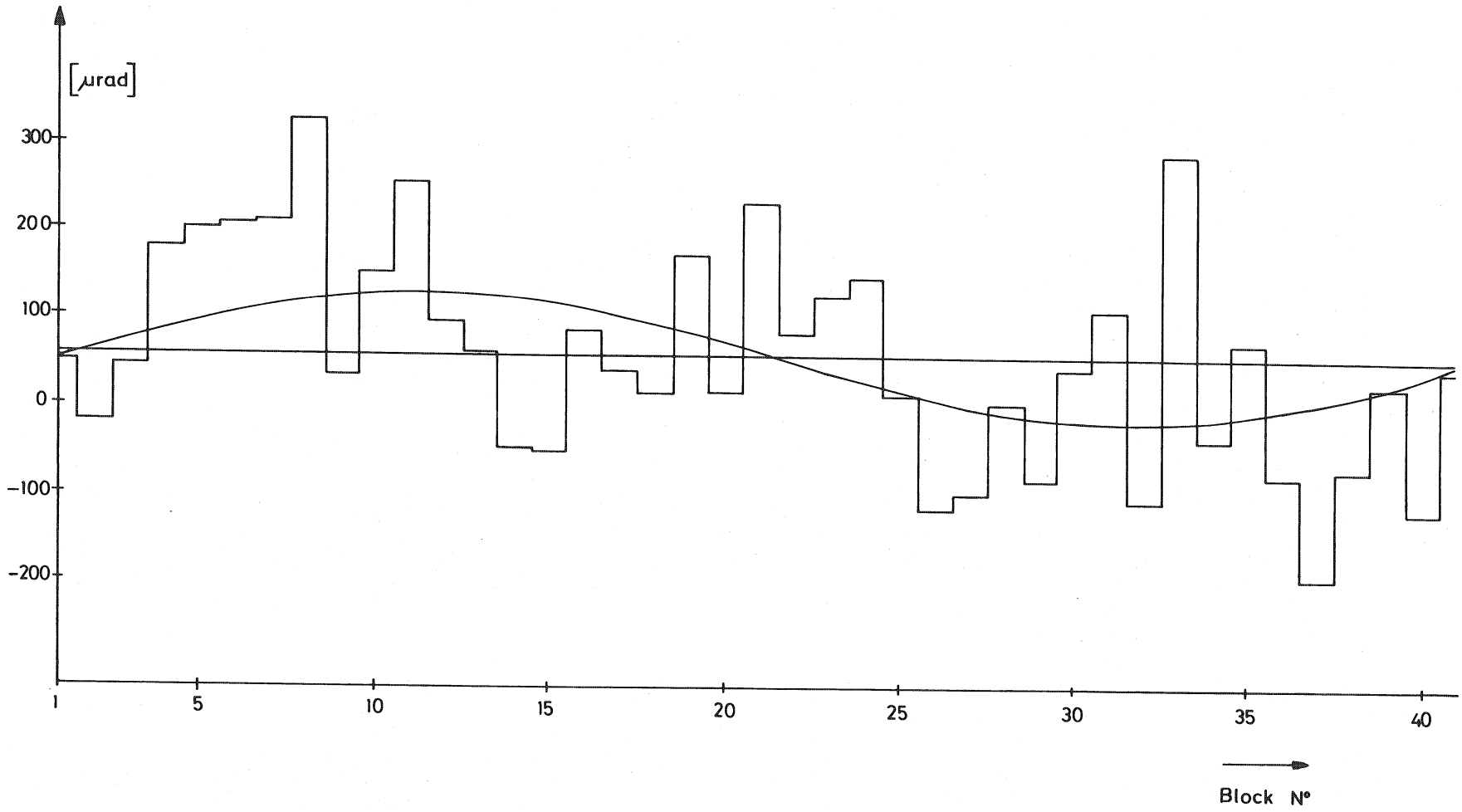

Fig. 14

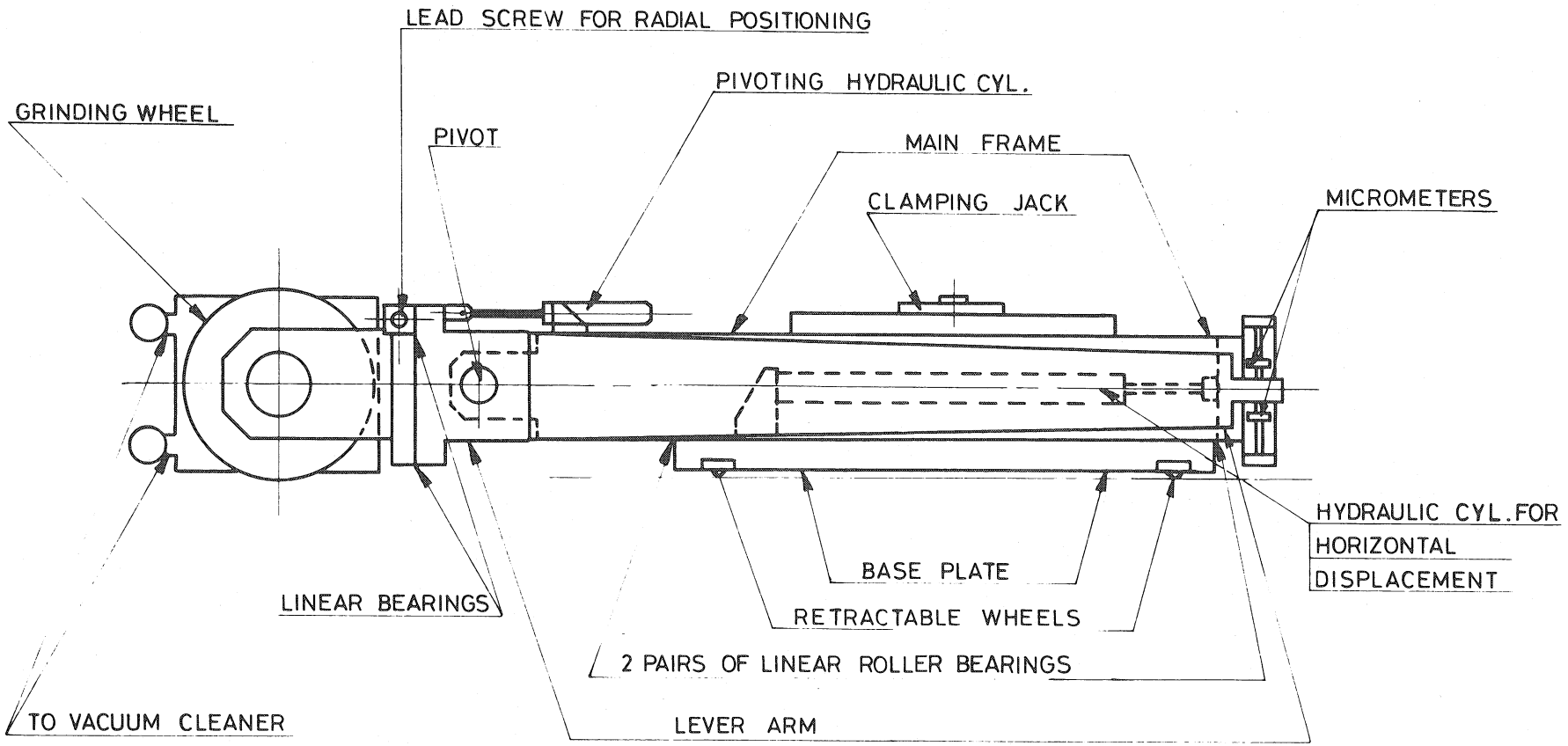
LEAD SCREW FOR RADIAL POSITIONING
PIVOTING HYDRAULIC CYL.
GRINDING WHEEL
PIVOT
MAIN FRAME
CLAMPING JACK
MICROMETERS
HYDRAULIC CYL. FOR
HORIZONTAL
DISPLACEMENT
BASE PLATE
LINEAR BEARINGS
RETRACTABLE WHEELS
2 PAIRS OF LINEAR ROLLER BEARINGS
TO VACUUM CLEANER
LEVER ARM

Fig. 15

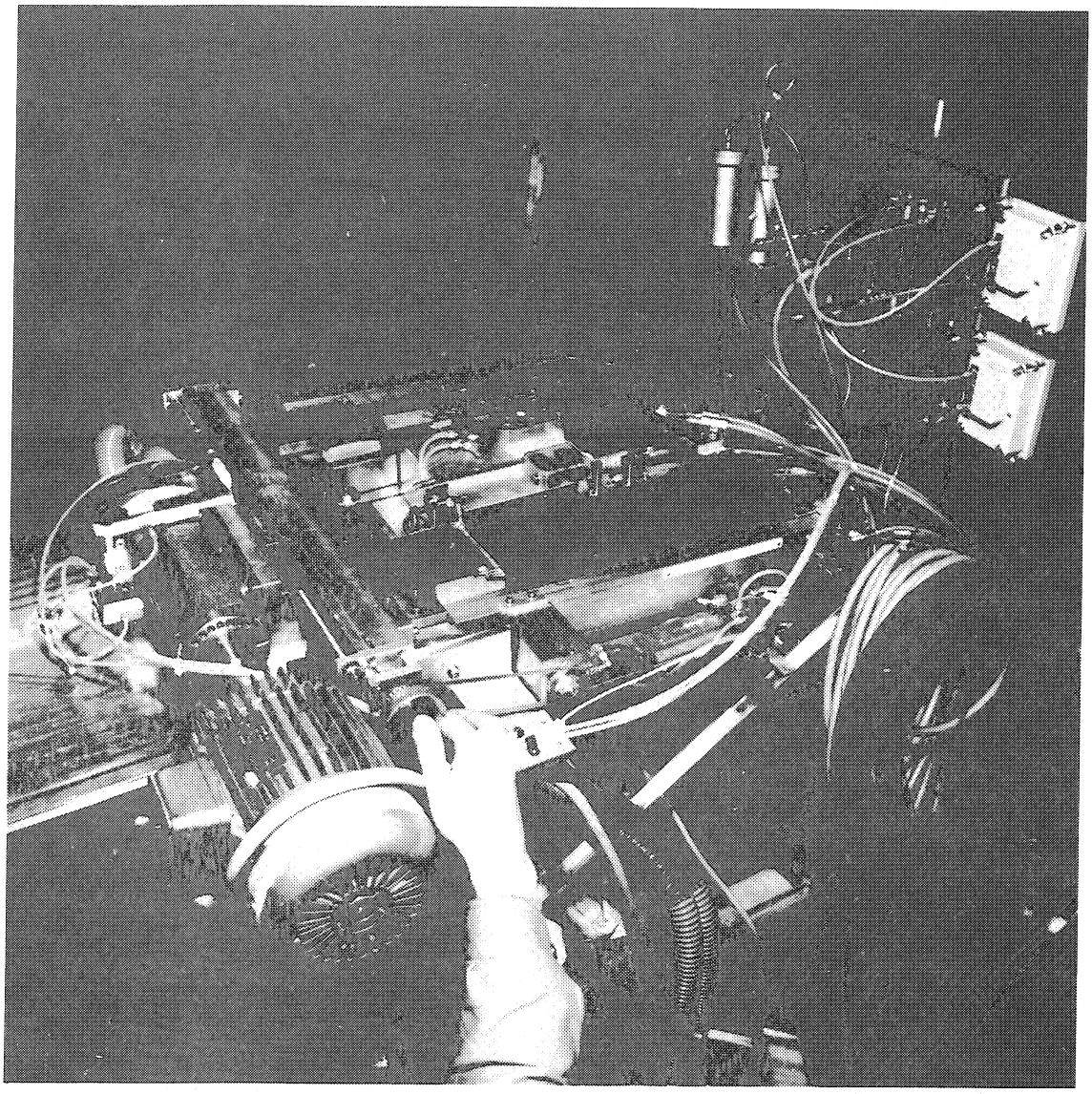

Fig. 16

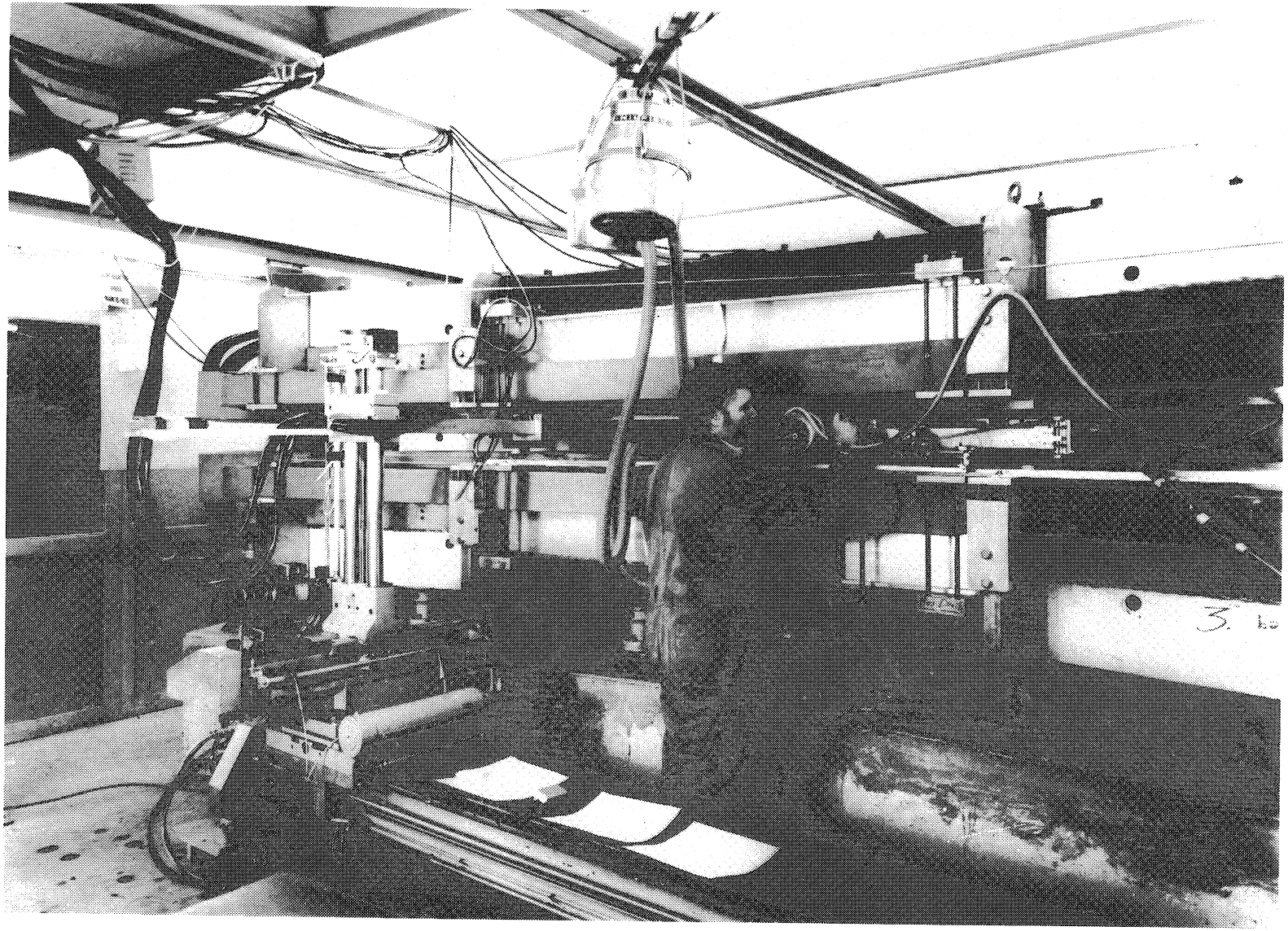

Fig. 17